The EMBO Journal Vol. 22 No. 3 pp. 395–403, 2003

C-terminal domains implicated in the functional surface expression of potassium channels

Marc Jenke[1], Araceli Sánchez, Francisco Monje, Walter Stühmer, Rüdiger M.Weseloh[2] and Luis A.Pardo[1,3]

Max Planck Institute for Experimental Medicine, Hermann-Rein-Straße 3, 37075 Göttingen, Germany

[1]Present address: iOnGen AG, Rudolf Wissell Straße 28, 37079 Göttingen, Germany
[2]Present address: Oppenheim Research GmbH, Unter Sachsenlausen 4, 50667 Köln, Germany

[3]Corresponding author
e-mail: lpardo@gwdg.de

R.M.Weseloh and L.A.Pardo contributed equally to this work

A short C-terminal domain is required for correct tetrameric assembly in some potassium channels. Here, we show that this domain forms a coiled coil that determines not only the stability but also the selectivity of the multimerization. Synthetic peptides comprising the sequence of this domain in Eag1 and other channels are able to form highly stable tetrameric coiled coils and display selective heteromultimeric interactions. We show that loss of function caused by disruption of this domain in Herg1 can be rescued by introducing the equivalent domain from Eag1, and that this chimeric protein can form heteromultimers with Eag1 while wild-type Erg1 cannot. Additionally, a short endoplasmic reticulum retention sequence closely preceding the coiled coil plays a crucial role for surface expression. Both domains appear to co-operate to form fully functional channels on the cell surface and are a frequent finding in ion channels. Many pathological phenotypes may be attributed to mutations affecting one or both domains.
Keywords: channelopathies/coiled coils/C-terminals/heteromultimeric interactions/ion-channel assembly

Introduction

Many voltage-gated potassium channels are tetramers composed of α subunits containing six transmembrane segments, generally termed S1–S6. A loop between S5 and S6 (P or H5 region) lines the permeability pathway. The group of genes possessing this conserved structure is termed 6TM1P (six transmembrane, one pore). α subunits encoded by different genes can also associate to form heterotetramers, adding an additional level of complexity to the system. As a general rule, heteromeric interactions are possible within closely related channels, but not between different families. The molecular determinants underlying the stability and selectivity of the interaction are only partially understood. In the first superfamily described among the 6TM1P channels, the Shaker-related (Kv) channels, a cytoplasmic N-terminal (T1) domain is involved in the assembly and has been characterized in detail (Li *et al*., 1992; Kreusch *et al*., 1998). Deletion of the T1 domain dramatically, but not completely, abolished channel formation. Interestingly, introduction of an artificial tetramerizing coiled coil can restore the function of these deletion mutants (Minor *et al*., 2000; Zerangue *et al*., 2000), indicating that coiled-coil structures can drive multimerization of ion channels.

Coiled coils are protein–protein interaction domains with a helical arrangement showing a heptad repeat $(abcdefg)_n$ where the positions *a* and *d* are preferably occupied by hydrophobic amino acids (Lupas, 1996). The amphipathic nature of this sequence drives the formation of multimers in an aqueous environment. Most natural coiled coils characterized to date correspond to dimers, although tetrameric structures have been reported in both artificial (Harbury *et al*., 1993) and naturally occurring molecules (Cupers *et al*., 1997; Fusetti *et al*., 1998; Hufton *et al*., 1998; Leclerc *et al*., 1998; Okamoto *et al*., 1999; Cabezon *et al*., 2000; Feng *et al*., 2000; O'Brien *et al*., 2000; Peng *et al*., 2000; Watanabe *et al*., 2000; Berggrun and Sauer, 2001; Cabezon *et al*., 2001; Stavolone *et al*., 2001).

Our laboratory has been interested in the structure and function of potassium channels of the EAG superfamily, including Eag1, Eag2 and HERG. In this group of channels, as well as in the related KCNQ channel family, deletion of a short domain near the C-terminus of the protein impairs tetramerization (Ludwig *et al*., 1997; Kupershmidt *et al*., 1998; Schmitt *et al*., 2000; Kupershmidt *et al*., 2002), indicating that a C-terminal domain, rather than an N-terminal T1 region, is required for subunit interaction. In Eag1, Erg1 and KCNQ1, the probability of the formation of a coiled-coil peaks in this domain, while it is very low in the rest of the protein. As mentioned above, a coiled-coil structure can drive the heteromerization of channels, at least under artificial conditions. Therefore we shall refer to this C-terminal domain as a 'tetramerizing coiled coil' (TCC).

Sequence-dependent factors (kinks, non-helical regions etc.) would confer specificity to the interaction and two different TCCs would not necessarily assemble in a stable manner; in other words, irregularities in the coiled coil can make the interaction specific. We present evidence here for specific interaction between TCCs both in synthetic peptides and within the whole channel molecule.

The C-terminal region of Erg1, and other channels (see below), contains, in addition to the TCC domain, an endoplasmic reticulum (ER) retention signal (RXR) that has been described to be relevant for functional expression in the plasma membrane (Kupershmidt *et al*., 2002). In fact, deletion of this sequence partially rescues functionality in TCC-deleted Erg1 channels. We tested the possible

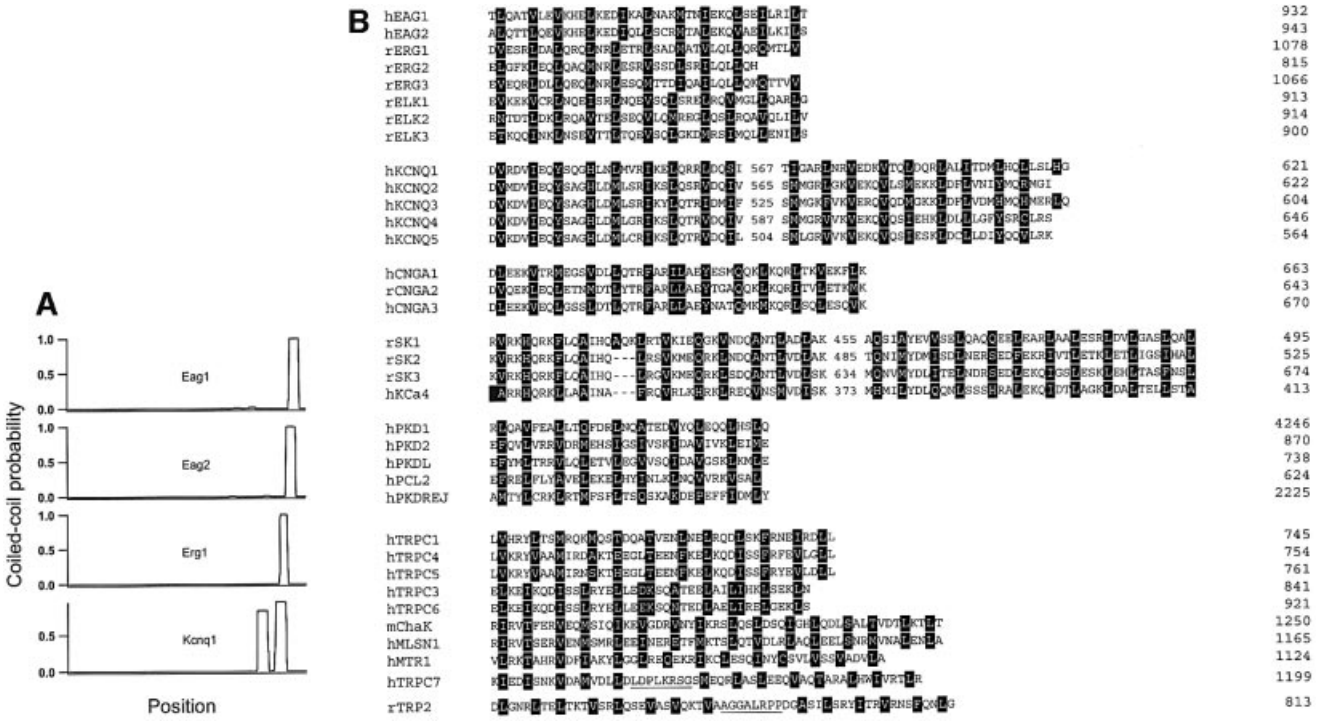

Fig. 1. (**A**) Coiled-coil probability for several 6TM1P ion channels. (**B**) Alignments of the amino acid sequences of TCC domains from different gene families. The domains corresponding to the KCNQ channels as well as the SK calcium channels, TRP2 and TRPC7 are bipartite [see (A) and text]. The first letter of the abbreviated names indicates the species [human (h), rat (r), or mouse (m)] and numbering refers to the position of the last depicted residue. Heptad positions *a* and *d* are emphasized (black boxes). Putative non-helical stretches are underlined.

cross-talk and relative contributions of the ER retention signal and of the TCC domain in functional channel assembly.

Results

TCC domains are a common structure in ion channels

A high probability for coiled-coil formation (Lupas *et al*., 1991) with features related to the TCC domains (see below) can be found in a variety of ion-channel sequences (Figure 1A). The TCC domain can be identified in such diverse gene families as cyclic nucleotide-gated cation channels (CNG) (Kaupp, 1991), voltage-gated potassium channels, in addition to Eag1 and Eag2, such as Elk (Warmke and Ganetzki, 1994; Engeland *et al*., 1998), Erg (Warmke and Ganetzki, 1994) and KCNQ (Biervert *et al*., 1998; Charlier *et al*., 1998; Kubisch *et al*., 1999), calcium-dependent potassium channels SK (Kohler *et al*., 1996) and IK (Ishii *et al*., 1997), non-selective cation channels (PKD) (Chen *et al*., 1999) and calcium channels (TRP) (Clapham *et al*., 2001). In most cases, the TCC is a continuous stretch of periodically repeated hydrophobic residues (Figure 1B), while for the KCNQ gene family, TRP2 and TRPC7, the TCC motif can be considered to be bipartite (Figure 1) owing to the presence of putatively helix-disruptive amino acids. In summary, a TCC motif appears not only to be present in a limited number of ion channels, but to represent a frequent feature of these proteins. Thus, we decided to investigate the functional properties of this domain.

Table I. Sequences of the peptides studied

TCCEag1	TLQATVLEVRHELKEDIKALNAKMTNIEK QLSEILRILTS
TCCEag2	ALQTTLQEVKHELKEDIQLLSCRMTALEK QVAEILKILS
TCCErg1	DVESRLDALQRQLNRLETRLSADMATVL QLLQRQMTLV
TCCEag1L20Y	TLQATVLEVRHELKEDIKAYNAKMTNIEK QLSEILRILTS
TCCEag2L13Y	ALQTTLQEVKHEYKEDIQLLSCRMTALEK QVAEILKILS
TCCErg1L20Y	DVESRLDALQRQLNRLETRYSADMATVL QLLQRQMTLV
TCCErgIns	RRGEQAGCPPAPAQQAGDPAECRHGHCPA AATEADDAG

Structure of TCC peptides

To test our predictions, we synthesized peptides encompassing the TCC domains of Eag1, Eag2 and Erg1 (Table I). A first prediction is that such peptides will form tetramers in solution. The stoichiometry of TCC peptides was initially assessed by size exclusion chromatography (SEC) (Figure 2A–C) to establish the apparent molecular weight (MW_{app}) of the peptides in solution. The MW_{app} was found to be 4.9 ± 0.3, 4.3 ± 0.2 and 4.4 ± 0.2 times the molecular weight of the monomer (MW_m) for TCCEag1, TCCEag2 and TCCErg1 respectively (Figure 2). This indicates that the monomers had assembled into tetramers. Under denaturing conditions, all peptides showed an MW_{app} of 1.5–1.6 times the MW_m (not shown).

To estimate the MW_{app} independently of secondary structure, we used SEC coupled to multi-angle laser light

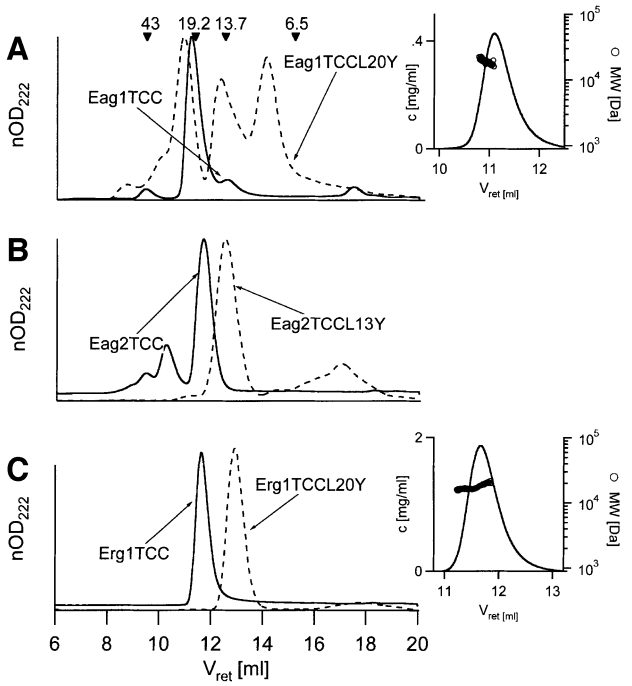

Fig. 2. Stoichiometry of TCC peptides. SEC performed under native conditions. The figures show normalized optical density (nOD) versus retention volume (V_{ret}) of (**A**) TCCEag1 (4591 Da, solid curve) and TCCEag1L20Y (broken curve), (**B**) TCCEag2 (4462 Da, solid curve) and TCCEag2L13Y (broken curve), and (**C**) TCCErg1 (4467 Da, solid curve) and TCCErg1L20Y (broken curve). Elution volumes corresponding to 43, 19.2, 13.7 and 6.5 kDa standards are marked by arrowheads. The insets to (A) and (C) show the determination of the apparent molecular weight under native conditions using MALLS. The concentration determined (left axis, solid curve) and the evaluated molecular weight (right axis, symbols) are plotted against the retention volume (V_{ret}).

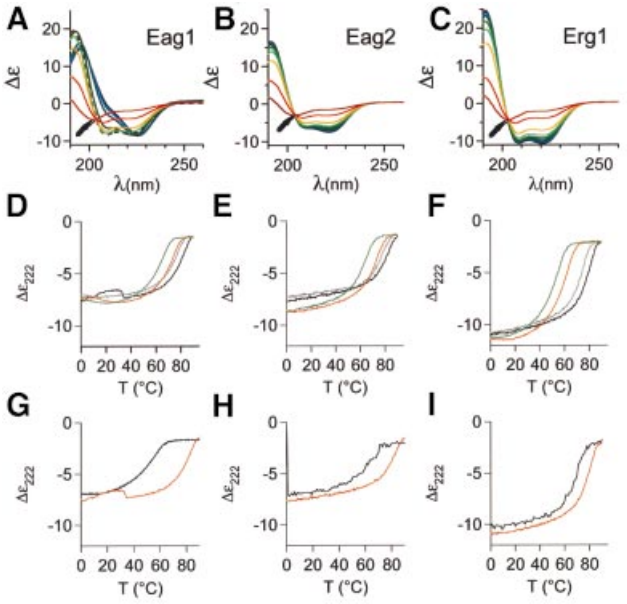

Fig. 3. Secondary structure and thermal stability of TCC peptides determined by CD spectroscopy. The temperature-dependent molar ellipticity (Δε) in the far UV from 190 to 260 nm of (**A**) TCCEag1, (**B**) TCCEag2 and (**C**) TCCErg1 is shown in 10°C increments from 0°C (dark blue) to 90°C (red). Note the nearly isodichroic point around 204 nm at all temperatures in the CD spectra of (B) TCCEag2 and (B) TCCERG1, as well as in (A) TCCEag1 at temperatures above 50°C (arrows; the spectrum corresponding to 50°C is represented by a broken curve). All peptides have a similar CD spectrum at 90°C, to which no defined protein structure can be assigned. (**D–F**) Molar ellipticities at 222 nm (Δε) of the thermal denaturation from 0 to 90°C (black) and the subsequent renaturation from 90 to 0°C (grey) in PBS and in 3.5 M guanidinium hydrochloride (red, green). (**G–I**) Molar ellipticities at 222 nm (Δε) of the thermal denaturation from 0 to 90°C of the mutant peptides (black) (G) TCCEagL20Y, (H) TCCEag2L13Y and (I) TCCErg1L20Y compared with those of the wild-type peptides from (D–F) (red).

scattering (MALLS) (Wyatt, 1993), shown in the insets to Figure 2A and C). Under non-denaturing conditions the MW_{app} were 18.8 ± 1.3 kDa for TCCEag1 and 17.5 ± 0.5 kDa for TCCErg1, corresponding to 4.1 ± 0.3 and 3.9 ± 0.1 times the MW_m and therefore also compatible with tetramerization of the peptides in solution.

The secondary structure and thermal stability of the peptides were tested by circular dichroism (CD) spectroscopy. CD wavelength scans (Figure 3) showed spectra compatible with a predominantly helical structure under physiological conditions. The helical content of the TCCEag1 peptide (Figure 3A) peaked at 40°C (83%), although the structural changes below that temperature were not homogeneous (data not shown). TCCEag2 and TCCErg1 (Figure 3B and C) were maximally helical at 0°C (76 and 91% respectively). The common value of Δε at ~204 nm in the CD spectra (TCCEag1 only above 50°C; Figure 3A) suggests the presence of only two detectable conformations, native and denatured. The melting points T_m of the native structure of the peptides in phosphate buffer were calculated to be 80°C for TCCEag1 (Figure 3D) and TCCEag2 (Figure 3E), and 79°C for TCCErg1 (Figure 3F), indicating a high stability of the native form of the peptide. The estimation of melting temperatures was not sufficiently accurate because denaturation was only complete at very high temperatures. To ensure complete denaturation below 90°C, we performed the same determinations in the presence of 3.5 M guanidinium hydrochloride (Figure 3D–F, coloured lines). Under such harsh denaturing conditions, the helical content at 0°C did not change significantly, but all the T_m values decreased (71, 69 and 59°C respectively); all denaturation profiles reached a plateau, confirming complete denaturation at 90°C, which was reversible in all cases.

Taken together, these results strongly suggest that TCC peptides form coiled coils which tetramerize with high stability. This observation would be compatible with the hypothesis that TCC domains are implicated in the multimerization of the entire channel protein.

We also synthesized mutant peptides with a single amino acid exchange at position *a* within the heptad repeat predicted to reduce the stability of the tetrameric coiled coil. The peptides were TCCEag1L20Y, TCCEag2L13Y and TCCErg1L20Y (Table I). The stoichiometry of these mutant peptides was not dramatically altered and apparently they were still able to form tetramers, although other stoichiometries were detected in significant amounts (Figure 2A–C, broken lines). However, the most dramatic effect was related to the stability of the coiled coil, as detected by CD spectroscopy. The melting points dropped from 80°C to 49, 60 and 68°C for Eag1, Eag2 and Erg1, respectively, strongly suggesting that the multimer stabil-

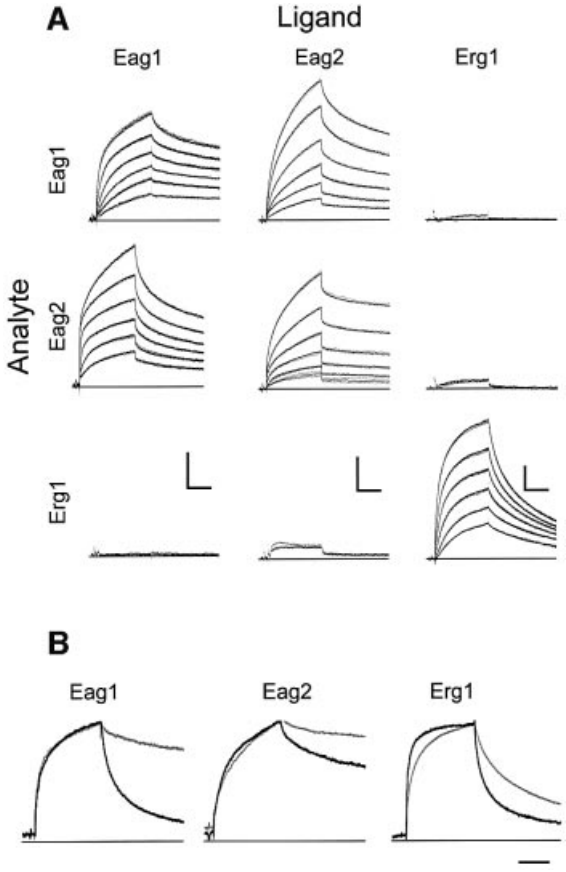

Fig. 4. (**A**) Kinetics of TCC peptide homo- and heteromeric assembly. Peptides were immobilized on the sensor surface (ligand, columns) and homomeric and heteromeric interactions were studied by surface plasmon resonance. Peptides in solution (analyte, rows) were brought into contact with the ligands for 480 s (association) and dissociation was monitored for 600 s (dots) at 1 Hz. When the injection of peptide at 3 μM yielded more than 5 RU, the interaction was studied in triplicate at decreasing concentrations of 3 μM, 1 μM, 300 nM, 100 nM, 30 nM and 10 nM, leading to decreasing responses. Fits are superimposed as solid lines. Scale bars: 200 s; 10 RU. (**B**) Kinetics of the heteromeric assembly of TCCEag1L20Y, TCCEag2L13Y and TCCErg1L20Y (as analytes) with the corresponding wild-type peptides (grey, as ligands). The corresponding homomeric interaction between wild-type peptides is shown in black. Scale bar: 200 s.

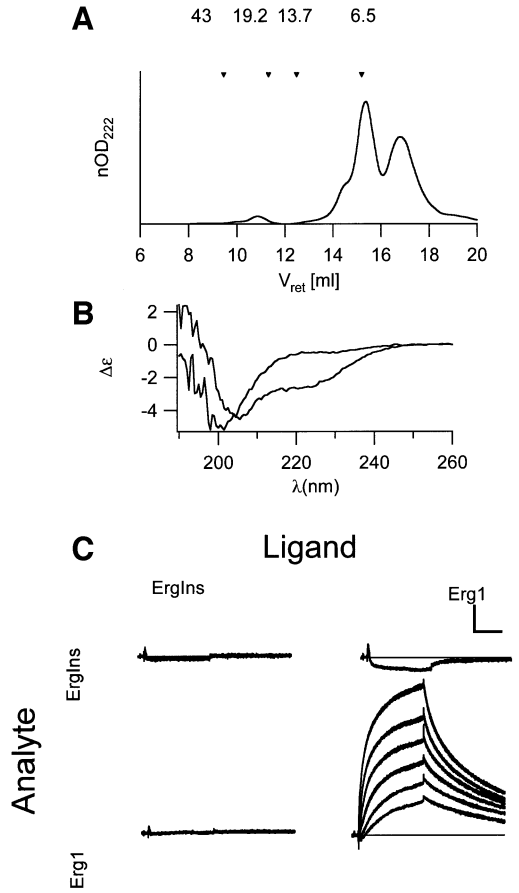

Fig. 5. Characterization of TCCErg1Ins peptide. (**A**) SEC under native conditions. Arrowheads mark the elution volumes of standard proteins. (**B**) Secondary structure measured by CD spectroscopy. The spectrum is not compatible with a helical structure. (**C**) Kinetics of TCCErgIns peptide assembly both in heteromeric interaction and with TCCErg1. Scale bars: 10 RU, 200 s.

ity is reduced by a mutation of a single amino acid at position *a* (Figure 3G–I).

Interaction between TCC peptides

We used surface plasmon resonance (SPR) to test the kinetics and specificity of the interaction between TCC peptides. Each of the individual peptides was coupled to the matrix, and the interaction between the immobilized peptide and a panel of peptides in solution was measured (Figure 4). The interaction measured is not a simple one-to-one binding, since the peptide used as an analyte (i.e. the circulating peptide) was equilibrated in solution prior to the interaction and therefore was in tetrameric form. Thus, we actually measured a competition between predominantly preformed tetramers and the monomers present on the surface.

All three peptides tested showed homomeric interactions with high stability (i.e. very slow off-rate), but a stable heteromeric interaction was only detected between TCCEag1 and TCCEag2 (Figure 4A). Thus, complexes of TCCEag1, TCCEag2 and TCCErg1 in solution discriminate between immobilized cognate peptides as opposed to peptides of other gene subfamilies, consistent with the behaviour described for the whole channel (Wimmers *et al.*, 2001). This result suggests that the TCC domain alone is sufficient to determine the specificity of assembly.

When the mutant peptides TCCEag1L20Y and TCCEag2L13Y were tested in the same experimental set-up, there was still a very significant interaction with the wild-type peptides but the affinity was greatly reduced, as indicated by a much faster dissociation (Figure 4B).

A naturally occurring Erg1 mutant lacks a TCC

We also synthesized a peptide corresponding to a naturally occurring TCC mutant in Erg1 channels (G insertion at position 3107; Splawski *et al.*, 2000) which underlies a form of the long-QT syndrome. This mutant should lack a TCC domain, since the frame shift renders a C-terminus whose secondary structure analysis does not predict a coiled coil.

The stoichiometry of the corresponding peptide (TCCErg1Ins) was determined by SEC, but no tetrameric structure was detected (Figure 5A). Furthermore, the peptide fails to form a coiled coil; its secondary structure is

dominated by either a random coil or a β-sheet, as determined by CD spectroscopy (Figure 5B).

In good agreement with these observations, the mutant peptide TCCErgIns did not show any interaction with Erg1 peptides (Figure 5C).

It is predicted that the channel carrying the mutation would not be able to give rise to functional Erg1 currents. The following experiments are in good agreement with this prediction.

Role of the TCC domain in subunit assembly and formation of functional channels

The results described above suggested that the TCC domain alone can drive selective tetramerization of the whole protein. To test this, we generated a mutant Erg1 channel (ErgIns) matching the naturally occurring insertion G at position 3107 (Splawski *et al*., 2000) and studied its functional expression in *Xenopus* oocytes. This mutant would correspond to the TCCErgIns peptide described above. We predicted that the channel would be non-functional because of the lack of a TCC. Indeed, we were unable to detect robust Erg1 currents in *Xenopus* oocytes injected with the mutant cRNA (Figure 6A and B).

To exclude the possibility that abnormal folding or incorrect subcellular distribution of the mutant channel accounted for the above result, we constructed a fusion protein consisting of Erg1 (either wild type or ErgIns) and the enhanced green fluorescent protein (EGFP) fused to its N-terminus. CHO cells transfected with either construct showed very similar fluorescence patterns (Figure 6C), suggesting that there are no dramatic differences in the distribution of the wild-type and the mutant channel. Most interestingly, EGFP:Erg1Ins shows a pattern consistent with partial localization to the plasma membrane.

It is evident from Figure 6B that both EGFP:Erg1 and EGFP:Erg1Ins give rise to a very strong intra-cytoplasmic label that might reflect ER retention. Recent work by Kupershmidt and coworkers has identified an ER retention signal (RXR) located near the C-terminal end of Erg1 (Kupershmidt *et al*., 2002). Mutation of this sequence led to functional channels even when the rest of the C-terminus had been truncated. We reproduced the double mutation annulating the ER retention signal in the Erg1Ins framework (Erg1Ins/LGL). When RNA coding for this construction was expressed in oocytes (Figure 6D and E), we found Erg1 currents several times larger than in the non-mutated truncation, confirming that the ER retention signal is partially responsible for the lack of functional expression after C-terminal deletion. Thus, the TCC domain is unlikely to be the only domain responsible for interaction, since some channels can form apparently functional tetramers without a TCC.

We then substituted the sequence downstream of the insertion in Erg1Ins for the Eag1 sequence containing its TCC domain, together with the 13 residues before and 28 after the putative TCC domain (chimera Erg1:Eag1TCC). RNA encoding this chimera was injected into oocytes (Figure 6D). The chimera was functional, and the current measured by two-electrode voltage–clamp showed the essential characteristic features of HERG channels, indicating that the C-terminal domain of Eag1 can promote the assembly of the Erg1 protein. This experiment does not unequivocally assign this function to the TCC domain, as

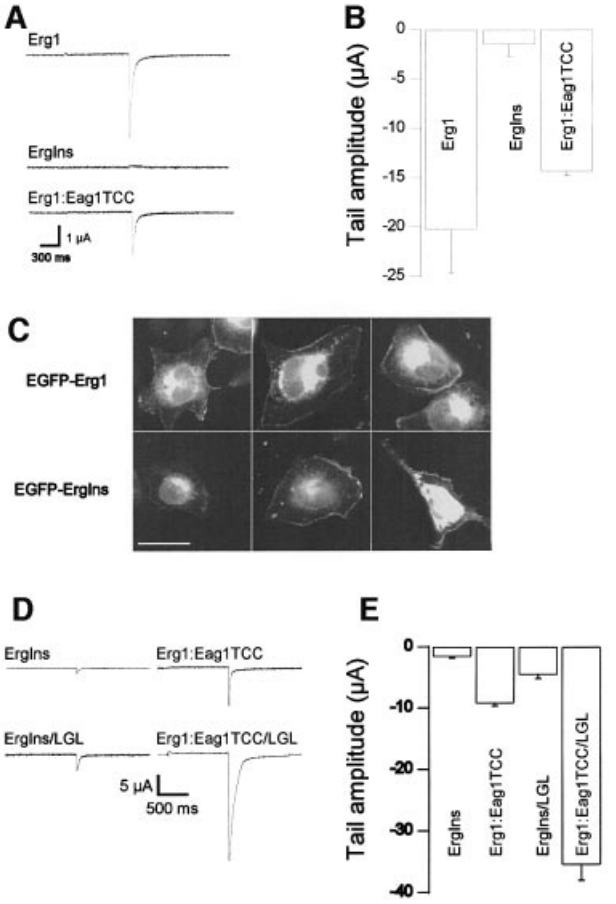

Fig. 6. (**A**) Disruption of the TCC domain in Erg1 by a frame shift (InsG3107) renders non-functional channels that are rescued by insertion of the Eag1TCC domain. Upper trace, Erg1 wild type; middle trace, ErgIns; lower trace, chimera ErgIns:Eag1TCC. (**B**) Mean tail current amplitudes in Erg1 ($N = 8$), ErgIns ($N = 21$) and ErgIns:Eag1TCC ($N = 20$) (Mean ± SEM). (**C**) EGFP fluorescence distribution of chimerical proteins EGFP-Erg1wt (upper row) and EGFP-ErgIns (lower row). Both show similar distribution with a significant portion of the fluorescence located at the plasma membrane. Scale bar: 25 µm. (**D**) Representative traces showing that LGL mutation gives rise to much larger currents in both the ErgIns and the ErgIns:Eag1TCC background. (**E**) Mean tail current amplitudes in ErgIns ($N = 21$), ErgIns/LGL ($N = 22$), ErgIns:Eag1TCC ($N = 22$) and ErgIns:Eag1TCC/LGL ($N = 19$). In these experiments, external potassium was 30 mM (mean ± SEM).

the chimerical protein contains residues before and after the putative TCC domain. However, we think it unlikely that the TCC flanking residues are responsible for the functional rescue of the mutant channel, as the TCC alone is known to be required for channel function in Eag1 (Ludwig *et al*., 1997).

To test the possibility that the addition of a TCC domain could lead to rescue of the current by masking the ER retention signal mentioned above and therefore leading to an improved trafficking of the channels rather than improved assembly, we also mutated the sequence RGR to LGL in the chimera. Expression of this channel led to robust currents, much larger than those of both the chimera with intact RGR and Erg1 wild type (Figure 6D and E). Thus, the effects of TCC addition and ER retention signal mutation are additive, strongly indicating that they are independent mechanisms. We were even forced to reduce

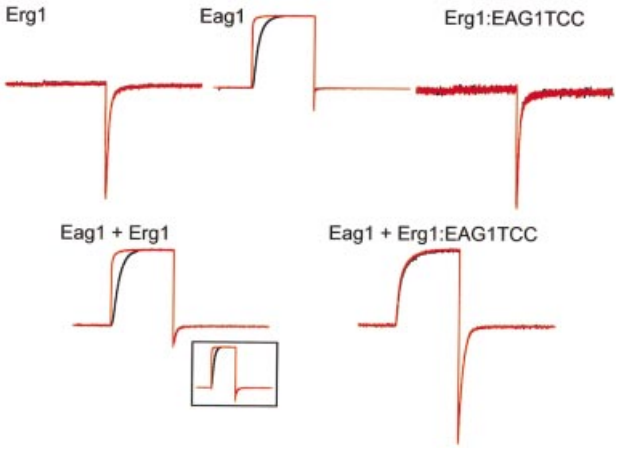

Fig. 7. Heteromeric interaction between Eag1 and Erg1:Eag1TCC. Currents were obtained in oocytes expressing wild-type Erg1, wild-type Eag1 or the chimera Erg1:Eag1TCC alone (upper traces), or co-expressing Eag1 + Erg1 or Eag1 + Erg1:Eag1TCC (lower traces). Current traces were obtained using a protocol designed to highlight both Eag1 and HERG properties which consisted of a long (5 s) pre-conditioning pulse to –140 mV (black traces) or –60 mV (red traces) followed by a depolarizing pulse to +60 mV for 1 s and a depolarization to –120 mV lasting for 1.5 s, and are shown after normalization to the maximal current value. Note the strong voltage dependence of the activation in Eag1 which is abolished in oocytes injected with Eag1+Erg1:Eag1TCC.

the extracellular potassium concentration from 70 to 30 mM in order to obtain a reasonable voltage control, owing to the size of the inward currents. Surprisingly, this reduction of external potassium alone led to an increase in the current amplitude of the ErgIns truncation (Figure 6).

Additionally, to test whether the TCC domain itself can determine the specificity of the subunit interaction, as suggested by our initial SPR experiments, we co-expressed the Erg1-Eag1TCC chimera with Eag1 wild-type channels in *Xenopus* oocytes (Figure 7). Eag1 and Erg1 channels, despite exhibiting a relative sequence similarity, have drastically different functional properties. The hallmark of Eag1 is a strong dependence of the activation kinetics on the potential prior to the stimulus (Ludwig *et al*., 1994; Terlau *et al*., 1996), while Erg1 currents are defined by a very fast inactivation that results in current flow only after the membrane potential is returned to the basal value (Trudeau *et al.*, 1995). We used these properties to identify each subfamily when testing for co-assembly. Eag1 and Erg1 are not able to form heteromultimers (Wimmers *et al*., 2001), and the current produced by co-expression of both channels in oocytes (Figure 7) can accurately be described by linear addition of the currents obtained when homomultimeric channels are expressed. The oocytes showed a whole-cell current with both a remarkable dependence on the membrane potential prior to the stimulus (conferred by the Eag1 channels) and a biphasic deactivation tail (from both types of channel). In contrast, when the Erg1:Eag1TCC chimerical protein was co-expressed with Eag1, the currents obtained clearly deviated from the predicted behaviour (Figure 7). The dependence on the pre-pulse potential was virtually abolished, and the tail current showed a monotonic decay, strongly indicating the formation of heteromultimeric channels with novel properties.

In summary, our data suggest that channel subunits whose TCC domains do not interact *in vitro* are unable to form functional heteromultimers at a detectable level *in vivo*. The introduction of compatible TCC domains has a permissive effect on the heteromeric interaction, thus highlighting the relevance of the TCC domain in determining the selectivity of subunit interaction.

Discussion

Our experiments provide evidence supporting the hypothesis that coiled-coil tetramerization can drive subunit interactions in many different ion channels, and also determines the specificity of interaction.

TCC domains form very stable tetramers. Structural differences between coiled coils that form either tetramers or dimers are to be expected. As the number of subunits increases, the hydrophobic core also needs to be larger to accommodate a greater number of hydrophobic side chains, and heptad positions *e* and *g* will become closer, with interactions between them becoming more important. Assuming a 100% accessibility of all side chains in a monomeric α-helix, ~87% of the side chains in positions *a* and *d*, as well as 26–27% of the side chains in positions *e* and *g*, would be buried in a dimer. For a tetramer, the respective values increase for positions *a* (92%) and *d* (99%) as well as for positions *e* (72%) and *g* (66%), as calculated for an artificial structure similar to the TCCs (Harbury *et al*., 1993). When we compared the heptad repeat of TCC sequences with that of dimeric coiled coils, which have been extensively characterized (O'Shea *et al*., 1989; Lupas *et al*., 1991), significant differences in the amino acid distribution were evident. There was no significant change in the frequency of occurrence of hydrophobic residues for the helical positions *b*, *c* and *f*, while in positions *a* and *d* the frequency of large hydrophobic residues increased from 60 and 50% respectively to 80% for both positions ($p < 0.001$). Conversely, alanine, the strongest helix stabilizing amino acid (O'Neil and DeGrado, 1990), is rarely found at TCC positions *a* (2%) and *d* (1%), whereas dimers quite frequently contain it (10%, $p < 0.05$; 22%, $p < 0.001$). Hence, the amino acid distribution in the TCCs is also compatible with tetramerization rather than dimerization. In contrast with dimerizing coiled coils, which are usually antiparallel, we assume a parallel orientation of the helices in TCC domains because they are derived from integral membrane proteins and therefore all subunits should be equally oriented. The putative *e–g* inter-helical interactions (i.e. hydrophobic–hydrophobic and positively charged–negatively charged residue pairs at opposing positions) also favour such an orientation.

The data presented here suggest that the ability of a particular channel subunit to form heteromultimers with those encoded by different genes is determined by compatibility of the TCC domains. In channels from the EAG superfamily, disruption of the TCC domain leads to non-functional channels, and introduction of a heterologous domain (Eag1 TCC) rescues the function, indicating that the presence of a TCC is enough to drive the formation of functional channels. Interactions between channels of the EAG superfamily and channels of the Kv family (the Shaker type, not containing a predicted TCC

domain) have been under debate for some time (Zhong and Wu, 1991, 1993; Brüggemann *et al*., 1993; Chen *et al.*, 1996, 2000; Tang *et al.*, 1998). Despite initial electrophysiological evidence suggesting co-assembly of both types of subunits, biochemical data have not supported a physical interaction. Our results reinforce the biochemical evidence, since heteromultimerization between 'carboxy-terminal' (like Eag) and 'amino-terminal' type channels (like Shaker) would expose hydrophobic areas in the TCC domains to the aqueous environment, and this would be energetically very unfavourable. The absence of a TCC dramatically impairs channel functional expression, but does not completely abolish it (see Kupershmidt *et al*., 2002; Figure 6). Under favourable conditions Erg1 channels lacking such a domain can give rise to small currents. Additionally, a HERG splice variant lacking the C-terminus ($HERG^{USO}$), although not functional when expressed alone, is capable of modifying the function of wild-type HERG when co-expressed, indicating the formation of heteromultimers (Kupershmidt *et al*., 1998). However, the presence of a TCC domain is the dominating factor driving the subunit assembly.

The recently described ER retention signal RGR at the C-terminal end of Erg1 also plays an important role in the correct maturation of the channel proteins. Thus, a truncated Erg1 can give rise to significant currents if the RGR sequence is deleted, although the size of the currents does not reach the wild-type levels. Additionally, when a TCC domain is added to the channel and the RGR sequence is mutated to LGL, the two effects combine to give rise to currents several-fold larger than those of wild type. It is interesting to note that wild-type Erg1 appears to be retained to a large extent in the ER of CHO cells, and also renders currents much smaller than our chimera Erg1-Eag1TCC/LGL. This suggests the intriguing possibility that, similarly to what has been described for other channels (Zerangue *et al*., 1999), Erg1 is not efficiently transported in heterologous cells owing to the lack of an accessory subunit that masks the RGR sequence in the native system.

Several TCC-bearing proteins are implicated in the pathogenesis of human diseases such as cardiac arrhythmia, epilepsy, deafness, visual dysfunction and renal disorders. If the TCC domain is essential for proper channel function, as our experiments indicate, any mutation altering its structure would result in significantly altered channel function and therefore produce symptoms. Hence, the TCC domain would be a 'hotspot' for mutations in patients suffering from channelopathies. We have identified at least 38 previously described mutations in seven different genes that affect the TCC domain of the respective products, i.e. mutations in (or close to) the TCC domains are much more frequent than a random distribution would predict (data available on request).

It is important to note that, whenever it has been tested, none of the mutant channels that completely lacked the TCC was functionally active. This is in good agreement with a model where the TCC domain mediates the subunit assembly of these channels. The frequent occurrence of mutations that affect the TCC domain, and consequently lead to channelopathies, highlights the crucial role of this domain for the formation of normally functional channels.

Materials and methods

Sequence analysis

The program Coils Version 2.2 (Lupas *et al*., 1991; http://www.ch.embnet.org) was used for the prediction of coiled-coil domains. The significance of changes in the amino acid distribution within the heptad repeats of dimeric and tetrameric coiled coils was calculated using the χ^2 test. Data for the amino acid distribution in the heptad repeats of coiled coils in dimeric proteins of the MTK type (Cohen and Parry, 1990) and the general frequency of amino acids in proteins published in GenBank were taken from Lupas *et al*. (1991). The LZ-type coiled coils of 217 transcription factors published in GenBank were aligned for maximal hydrophobicity at heptad positions *a* and *d* prior to analysis. The TCC domains used in the analysis are shown in Figure 1: Eag1, 2 (DDBJ/EMBL/GenBank accession Nos AF078741, EST-Klon U69185), Erg1-3 (CAB09536, AAB94742, AAB94741), Elk1-3 (CAA07587, CAA07586, AAC61520), KCNQ1-5 (AAC51776, CAA75348, AAB97314, AAD14681, AAF73446), CNGAA1-3 (P29973, Q00195, AAC17440), SK1-3 (AAB82740, AAB09563, AAB81653), KCa4 (AAC51913), PKD1, 2, L, REJ (AAB59488, AAC16004, AAD41638, AAD18021), PCL2 (AAF65622), TRPC1, 3–7 (CAA61447, AAC51653, AAD51736, AAF00002, AAC63289, BAA95563), hMTR1 (AAF26288), mChaK (AAF73131), hMLSN1 (AAC80000) and TRP2 (AAD31453). Additionally, homologues of the proteins from different species available in GenBank and tetrameric coiled coils of BCR/abl (26–65, accession No. AAA35594) and viral proteins (Leclerc *et al*., 1998) were included in the analysis.

Chromatography and MALLS

Peptides were synthesized and purified, and were N-terminal acetylated and C-terminal amidated to avoid the introduction of additional charges (sequences are listed in Table I). Peptide sequences were checked by MALDI-TOF mass spectrometry: 1 mg/ml corresponded to 0.13 mM (TCCEag1), 0.30 mM (TCC Eag1L20Y), 0.21 mM (TCCEag2), 0.26 mM (TCCEag2L13Y), 0.16 mM (TCCErg1), 0.33 mM (TCCErg1L20Y) and 0.4 mM (TCCErgIns) as determined by amino acid analysis. Molecular weight determination of peptide complexes in solution was performed on a size exclusion chromatography (SEC) column (HR-10/30 Superdex 75 column, Pharmacia Biotech). Either PBS (native conditions) or PBS plus 6 M guanidinium hydrochloride (denaturing conditions) was used as running buffer. The same conditions were used to calibrate the column at either condition with ovalbumin (43 kDa), chymotrypsinogen A (19.2 kDa), ribonuclease A (13.7 kDa) and aprotinin (6.5 kDa). Under denaturing conditions, protein kinase A inhibitor (2.2 kDa) and vitamin B12 (1.4 kDa) were added for calibration. Alternatively, molecular weight determination was carried out by monitoring the light-scattering signal of the SEC eluent at 18 different angles and the differential refractive index, both at 632.8 nm (DAWN DSP laser photometer and Optilab DSP interferometric refractometer, Wyatt Technology, Santa Barbara, CA), as well as the optical density at 280 nm. Data analysis was carried out using the program Astra (Wyatt) with a constant d*n*/d*c* value of 0.189.

Circular dichroism

Far UV CD spectra from 190 to 260 nm (in steps of 1 nm) were obtained by averaging five to ten scans on a CD spectrometer (Jasco JA 720 and PTC-315). The recordings of 1 mg/ml peptide in either PBS or 3.5 M guanidinium hydrochloride in PBS were performed using Suprasil cuvettes (Hellma) with a path length of 0.2 cm. The helical content of the peptides was evaluated by deconvolution of the spectra using CDNN (Bohm *et al*., 1992; bioinf1.biochemtech.uni-halle.de). The thermal stability of the peptides was measured by monitoring the ellipticity at 222 nm ($\Delta\varepsilon_{222}$), denaturing from 0 to 90°C and subsequently renaturing from 90 to 0°C (2°C/min). Melting points (T_m) were calculated from the average of the maximal slope of the recorded denaturing and renaturing temperature-dependent $\Delta\varepsilon_{222}$.

Surface plasmon resonance

Experiments were performed on a BIAcore 2000 system (Biacore). For covalent immobilization the TCC peptides (ligand) were diluted to 1.3–3.2 μM in 10 mM acetate buffer pH 4.0 or 4.5, and coupled via primary amines. Owing to the lack of lysine in the TCC ERG1 peptide, an N-terminal unmodified peptide was used for immobilization. Each analyte–ligand pair was first examined for interaction at an analyte concentration of 3 μM. Interacting analyte–ligand pairs (>5 RU after 480 s, 3 μM) were subsequently analysed at concentrations from 10 nM to

3 μM. Traces of interacting peptides are averages of three injections. Data from a reference sensor surface without immobilized peptide were subtracted before analysis.

Molecular biology

Site-directed mutagenesis was performed using the QuikChange XL Site-Directed Mutagenesis kit (Stratagene, Amsterdam, The Netherlands) following the protocol recommended by the manufacturer. All mutants were fully sequenced to avoid the risk of additional mutations introduced in PCR. To generate the Erg1:Eag1TCC chimera, an *Asc*I site was introduced in both sequences (position 3002 in Erg1 and position 2680 in Eag1) and a fragment *Asc*I–*Bam*HI was transferred from Eag1 into the ErgIns backbone.

The EGFP:Erg1 and EGFP:ErgIns were generated inserting a fragment *Eco*RI–*Hin*dIII in the pEGFPC3 vector from Invitrogen (Karlsruhe, Germany). Transient transfection of CHO K1 cells was performed using DAC30 (Eurogentec, Seraing, Belgium) in a ration of 2.5:1 with DNA, and the cells were observed and photographed by conventional epifluorescence and confocal microscopy both *in vivo* and after fixation with 4% *p*-formaldehyde.

For electrophysiological experiments, cRNAs synthesized using standard protocols (Krieg and Melton, 1987), were injected (or co-injected) into oocytes from *Xenopus laevis* as described previously (Stühmer, 1992).

Electrophysiology

Currents were recorded 1–7 days after cRNA injection using a Turbo TEC -10CD amplifier (npi Electronics, Tamm, Germany). Intracellular electrodes had resistances of 0.6–1 MΩ when filled with 2 M KCl. Recordings were obtained at room temperature in an external solution containing 85 mM NaCl, 30 mM KCl, 1.8 mM $CaCl_2$, 2.0 mM $MgCl_2$ and 10 mM HEPES–NaOH pH 7.2. On-line leak subtraction was systematically performed using a P/n protocol. Data were acquired and analysed using Pulse-PulseFit (HEKA Electronics, Lambrecht, Germany) and IGOR Pro (WaveMetrics, Inc. Lake Oswego, OR) software packages.

Acknowledgements

We thank Dr R.García for help with electrophysiological experiments and for helpful discussions, Drs O.Brauns, K.Eckart and C.Morys-Wortmann (Max Planck Institute for Experimental Medicine) for peptide synthesis, Drs V.Subramaniam and D.Fasshauer (Max Planck Institute for Biophysical Chemistry) for help with the CD spectroscopy, Professor G.Mieskes and Dr S.Pabst (Max Planck Institute for Biophysical Chemistry) for help with the MALLS, A.Suckow for helpful discussions, and Drs S.Smith and H.Knötgen for critically reading the manuscript. F.M. wishes to thank Dr E.Posada, Dr M.Camacho, Ms I.Rugeles and Dr E.Rey (CIF) and COLCIENCIAS for support. F.M. was supported by Centro Internacional de Física (CIF), Colombia.

References

Berggrun,A. and Sauer,R.T. (2001) Contributions of distinct quaternary contacts to cooperative operator binding by Mnt repressor. *Proc. Natl Acad. Sci. USA*, **98**, 2301–2305.

Biervert,C., Schroeder,B.C., Kubisch,C., Berkovic,S.F., Propping,P., Jentsch,T.J. and Steinlein,O.K. (1998) A potassium channel mutation in neonatal human epilepsy. *Science*, **279**, 403–406.

Bohm,G., Muhr,R. and Jaenicke,R. (1992) Quantitative analysis of protein far UV circular dichroism spectra by neural networks. *Protein Eng.*, **5**, 191–195.

Brüggemann,A., Pardo,L.A., Stühmer,W. and Pongs,O. (1993) *Ether-à-go-go* encodes a voltage-gated channel permeable to K^+ and Ca^{2+} and modulated by cAMP. *Nature* **365**, 445–448.

Cabezon,E., Arechaga,I., Butler,P.J.G. and Walker,J.E. (2000) Dimerization of bovine F-1-ATPase by binding the inhibitor protein, IF1. *J. Biol. Chem.*, **275**, 28353–28355.

Cabezon,E., Runswick,M.J., Leslie,A.G.W. and Walker,J.E. (2001) The structure of bovine IF1, the regulatory subunit of mitochondrial F-ATPase. *EMBO J.*, **20**, 6990–6996.

Charlier,C., Singh,N.A., Ryan,S.G., Lewis,T.B., Reus,B.E., Leach,R.J. and Leppert,M. (1998) A pore mutation in a novel KQT-like potassium channel gene in an idiopathic epilepsy family. *Nat. Genet.*, **18**, 53–55.

Chen,M.L., Hoshi,T. and Wu,C.F. (1996) Heteromultimeric interactions among K^+ channel subunits from *shaker* and *eag* families in *Xenopus* oocytes. *Neuron*, **17**, 535–542.

Chen,M.L., Hoshi,T. and Wu,C.F. (2000) Sh and Eag K^+ channel subunit interaction in frog oocytes depends on level and time of expression. *Biophys. J.*, **79**, 1358–1368.

Chen,X.Z. *et al.* (1999) Polycystin-L is a calcium-regulated cation channel permeable to calcium ions. *Nature*, **401**, 383–386.

Clapham,D.E., Runnels,L.W. and Strubing,C. (2001) The TRP ion channel family. *Nat. Rev. Neurosci.*, **2**, 387–396.

Cohen,C. and Parry,D.A. (1990) α-helical coiled coils and bundles: how to design an α-helical protein. *Proteins*, **7**, 1–15.

Cupers,P., Terhaar,E., Boll,W. and Kirchhausen,T. (1997) Parallel dimers and anti-parallel tetramers formed by epidermal growth factor receptor pathway substrate clone 15 (eps15). *J. Biol. Chem.*, **272**, 33430–33434.

Engeland,B., Neu,A., Ludwig,J., Roeper,J. and Pongs,O. (1998) Cloning and functional expression of rat ether-a-go-go-like K^+ channel genes. *J. Physiol.*, **513**, 647–654.

Feng,B., Haas,H. and Marzluf,G.A. (2000) ASD4, a new CATA factor of *Neurospora crassa*, displays sequence-specific DNA binding and functions in ascus and ascospore development. *Biochemistry*, **39**, 11065–11073.

Fusetti,F., Erlandsen,H., Flatmark,T. and Stevens,R.C. (1998) Structure of tetrameric human phenylalanine hydroxylase and its implications for phenylketonuria. *J. Biol. Chem.*, **273**, 16962–16967.

Harbury,P.B., Zhang,T., Kim,P.S. and Alber,T. (1993) A switch between two-, three- and four-stranded coiled coils in GCN4 leucine zipper mutants. *Science*, **262**, 1401–1407.

Hufton,S.E., Jennings,I.G. and Cotton,R.G.H. (1998) Structure/function analysis of the domains required for the multimerisation of phenylalanine hydroxylase. *Biochim. Biophys. Acta*, **1382**, 295–304.

Ishii,T.M., Silvia,C., Hirschberg,B., Bond,C.T., Adelman,J.P. and Maylie,J. (1997) A human intermediate conductance calcium-activated potassium channel. *Proc. Natl Acad. Sci. USA*, **94**, 11651–11656.

Kaupp,U.B. (1991) The cyclic nucleotide- gated channels of vertebrate photoreceptors and olfactory epithelium. *Trends Neurosci.*, **14**, 150–157.

Kohler,M., Hirschberg,B., Bond,C.T., Kinzie,J.M., Marrion,N.V., Maylie,J. and Adelman,J.P. (1996) Small-conductance, calcium-activated potassium channels from mammalian brain. *Science*, **273**, 1709–1714.

Kreusch,A., Pfaffinger,P.J., Stevens,C.F. and Choe,S. (1998) Crystal structure of the tetramerization domain of the Shaker potassium channel. *Nature*, **392**, 945–948.

Krieg,P.A. and Melton,D.A. (1987) *In vitro* RNA synthesis with SP6 RNA polymerase. *Methods Enzymol.*, **155**, 397–415.

Kubisch,C., Schroeder,B.C., Friedrich,T., Lutjohann,B., El-Amraoui,A., Marlin,S., Petit,C. and Jentsch,T.J. (1999) KCNQ4, a novel potassium channel expressed in sensory outer hair cells, is mutated in dominant deafness. *Cell*, **96**, 437–446.

Kupershmidt,S., Snyders,D.J., Raes,A. and Roden,D.M. (1998) A K^+ channel splice variant common in human heart lacks a C-terminal domain required for expression of rapidly activating delayed rectifier current. *J. Biol. Chem.*, **273**, 27231–27235.

Kupershmidt,S., Yang,T., Chanthaphaychith,S., Wang,Z.Q., Towbin,J.A. and Roden,D.M. (2002) Defective human *ether-a-go-go*-related gene trafficking linked to an endoplasmic reticulum retention signal in the C terminus. *J. Biol. Chem.*, **277**, 27442–27448.

Leclerc,D., Burri,L., Kajava,A.V., Mougeot,J.L., Hess,D., Lustig,A., Kleemann,G. and Hohn,T. (1998) The open reading frame III product of cauliflower mosaic virus forms a tetramer through a N-terminal coiled-coil. *J. Biol. Chem.*, **273**, 29015–29021.

Li,M., Jan,Y.N. and Jan,L.Y. (1992) Specification of subunit assembly by the hydrophilic amino-terminal domain of the Shaker potassium channel. *Science*, **257**, 1225–1230.

Ludwig,J., Terlau,H., Wunder,F., Brüggemann,A., Pardo,L.A., Marquardt,A., Stühmer,W. and Pongs,O. (1994) Functional expression of a rat homologue of the voltage gated ether a go-go potassium channel reveals differences in selectivity and activation kinetics between the *Drosophila* channel and its mammalian counterpart. *EMBO J.*, **13**, 4451–4458.

Ludwig,J., Owen,D. and Pongs,O. (1997) Carboxy-terminal domain mediates assembly of the voltage-gated rat ether-a-go-go potassium channel. *EMBO J.*, **16**, 6337–6345.

Lupas,A. (1996) Coiled coils: new structures and new functions. *Trends Biochem. Sci.*, **21**, 375–382.

Lupas,A., Van Dyke,M. and Stock,J. (1991) Predicting coiled coils from protein sequences. *Science*, **252**, 1162–1164.

Minor,D.L., Lin,Y.F., Mobley,B.C., Avelar,A., Jan,Y.N., Jan,L.Y. and Berger,J.M. (2000) The polar T1 interface is linked to conformational changes that open the voltage-gated potassium channel. *Cell*, **102**, 657–670.

O'Brien,J.A., Taylor,J.A. and Bellamy,A.R. (2000) Probing the structure of rotavirus NSP4: a short sequence at the extreme C terminus mediates binding to the inner capsid particle. *J. Virol.*, **74**, 5388–5394.

Okamoto,P.M., Tripet,B., Litowski,J., Hodges,R.S. and Vallee,R.B. (1999) Multiple distinct coiled-coils are involved in dynamin self-assembly. *J. Biol. Chem.*, **274**, 10277–10286.

O'Neil,K.T. and DeGrado,W.F. (1990) A thermodynamic scale for the helix-forming tendencies of the commonly occurring amino acids [published erratum appears in *Science*, **253**, 952]. *Science*, **250**, 646–651.

O'Shea,E.K., Rutkowski,R. and Kim,P.S. (1989) Evidence that the leucine zipper is a coiled coil. *Science*, **243**, 538–542.

Peng,H.Z., Begg,G.E., Schultz,D.C., Friedman,J.R., Jensen,D.E., Speicher,D.W. and Rauscher,F.J. (2000) Reconstitution of the KRAB-KAP-1 repressor complex: a model system for defining the molecular anatomy of RING-B box-coiled-coil domain-mediated protein–protein interactions. *J. Mol. Biol.*, **295**, 1139–1162.

Schmitt,N., Schwarz,M., Peretz,A., Abitbol,I., Attali,B. and Pongs,O. (2000) A recessive C-terminal Jervell and Lange–Nielsen mutation of the KCNQ1 channel impairs subunit assembly. *EMBO J.*, **19**, 332–340.

Splawski,I. *et al.* (2000) Spectrum of mutations in long-QT syndrome genes KVLQT1, HERG, SCN5A, KCNE1 and KCNE2. *Circulation*, **102**, 1178–1185.

Stavolone,L., Herzog,E., Leclerc,D. and Hohn,T. (2001) Tetramerization is a conserved feature of the virion-associated protein in plant pararetroviruses. *J. Virol.*, **75**, 7739–7743.

Stühmer,W. (1992) Electrophysiological recordings from *Xenopus* oocytes. *Meth. Enzymol.*, **207**, 319–339.

Tang,C.Y., Schulteis,C.T., Jimenez,R.M. and Papazian,D.M. (1998) *Shaker* and ether-a-go-go K^+ channel subunits fail to coassemble in *Xenopus* oocytes. *Biophys. J.*, **75**, 1263–1270.

Terlau,H., Ludwig,J., Steffan,R., Pongs,O., Stühmer,W. and Heinemann,S.H. (1996) Extracellular Mg^{2+} regulates activation of rat eag potassium channel. *Pflugers Arch.*, **432**, 301–312.

Trudeau,M.C., Warmke,J.W., Ganetzky,B. and Robertson,G.A. (1995) HERG, a human inward rectifier in the voltage-gated potassium channel family. *Science*, **269**, 92–95.

Warmke,J.W. and Ganetzki,B. (1994) A family of potassium channel genes related to *eag* in *Drosophila* and mammals. *Proc. Natl Acad. Sci. USA*, **91**, 3438–3442.

Watanabe,S., Take,H., Takeda,K., Yu,Z.X., Iwata,N. and Kajigaya,S. (2000) Characterization of the CIN85 adaptor protein and identification of components involved in CIN85 complexes. *Biochem. Biophys. Res. Commun.*, **278**, 167–174.

Wimmers,S., Wulfsen,I., Bauer,C.K. and Schwarz,J.R. (2001) Erg1, erg2 and erg3 K channel subunits are able to form heteromultimers. *Pflugers Arch.*, **441**, 450–455.

Wyatt,P.J. (1993) Light scattering and the absolute characterization of macromolecules. *Anal. Chim. Acta*, **272**, 1–40.

Zerangue,N., Schwappach,B., Jan,Y.N. and Jan,L.Y. (1999) A new ER trafficking signal regulates the subunit stoichiometry of plasma membrane K-ATP channels. *Neuron*, **22**, 537–548.

Zerangue,N., Jan,Y.N. and Jan,L.Y. (2000) An artificial tetramerization domain restores efficient assembly of functional Shaker channels lacking T1. *Proc. Natl Acad. Sci. USA*, **97**, 3591–3595.

Zhong,Y. and Wu,C.F. (1991). Alteration of four identified K^+-currents in *Drosophila* muscle by mutations in *eag*. *Science*, **252**, 1562–1564.

Zhong,Y. and Wu,C.F. (1993). Modulation of different K^+-currents in *Drosophila*—a hypothetical role for the *eag* subunit in multimeric K^+-channels. *J. Neurosci.* **13**, 4669–4679.

Received June 27, 2002; revised November 8, 2002; accepted November 22, 2002